Applications of combined EXAFS and powder diffraction analysis in solid state chemistry

Norman Binsted,[a*] Marit Stange,[b] Craig Owens,[a] Helmer Fjellvåg[b] and Mark T. Weller[a]

[a]Department of Chemistry, University of Southampton, Southampton SO17 1BJ, England, [b]Department of Chemistry, University of Oslo, N-0315 Oslo, Norway. E-mail: N.Binsted@dl.ac.uk.

Recent applications of combined EXAFS/powder neutron and X-diffraction analysis are reviewed and provisional results for three additional compounds are presented. Criteria for successful refinements are suggested. The new results relate to the materials: $CoAl_2O_4$, $La_{6.4}Ca_{1.6}Cu_6Ni_2O_{20}$ and $Pr_{0.5}Sr_{0.5}FeO_{2.75}$.

Keywords: EXAFS, powder diffraction, combined refinement.

1. Introduction

Although the characterisation of the products of solid-state synthesis relies heavily on powder diffraction methods, many other techniques are used in conjunction in order to provide a complete description of the structure. In particular, EXAFS provides details of the local structure inaccessible to diffraction methods. Although a unique description of the structure from EXAFS alone may be possible for small molecular species in solution, it is certainly not for the majority of crystalline materials. Indeed, it may not even be possible to resolve nearest neighbour distances, as in many materials of interest to solid state chemists, a metal may occupy several distorted sites, and splitting of the oxygen shells cannot be reliably determined due to correlations with the Debye-Waller (DW) terms. Combined EXAFS/Powder Diffraction (PD) analysis (Binsted *et al*., 1996) provides the ideal way of resolving these difficulties, providing an improved overall description of the structure. The need for both a local and long-range description of the structure was highlighted in a recent study of $Gd_2Ba_2CaCu_2Ti_3O_{14}$, in which the five metal EXAFS spectra and the PND profile were refined simultaneously (Weller *et al*., 1996). Neither of the sites were accurately described by the long-range structural model and anomalies were large for the Ca and Ti sites. In such cases, both techniques are required in order to develop and refine structural models. The modelling of structures where the local and long-range structures disagree can be challenging. In a study of the framework silicate Gallobicchulite, $Ca_8Ga_8Si_4O_{24}(OH)_8$ (Binsted *et al*., 1998), a single set of positional parameters was used to model a structure with ordered domains, using two different space groups (with partial PD occupancies for the higher-symmetry long-range space group). This approach has been found to be very useful where cation positions are locally ordered. It has been used in $La_{6.4}Ca_{1.6}Cu_7CoO_{20}$ (Binsted *et al*., 2001), a compound closely related to the $La_{6.4}Ca_{1.6}Cu_6Ni_2O_{20}$ example below. Where some or all of the cation positions are randomly occupied, and resulting lattice distortions are large, this approach is less valid. In such cases, the use of the reverse Monte-Carlo method (McGreevy, 1995) is appropriate.

2. Experimental

Spinels were synthesised from oxides at 1400 K. Fully oxidized perovskite derivatives were prepared from metal oxides, acetates or metals, in acid solution. $La_{6.4}Ca_{1.6}Cu_6Ni_2O_{20}$ was annealed in oxygen for 48 hours at 1298 K and $Pr_{0.5}Sr_{0.5}FeO_{3-\delta}$ was annealed in nitrogen for 48 hours at 1430 K and then in air for 24 hours at 1173 K before it was reduced to $Pr_{0.5}Sr_{0.5}FeO_{2.75}$ by Zr metal at 1073 K. Spinel tof neutron data were collected at the polaris diffractometer, ISIS. X-ray image-plate data were recorded at SRS station 9.1. For the perovskites, fixed-wavelength powder neutron diffraction measurements were made at the JEEPII reactor, Kjeller, Norway, using wavelengths from 1.5554 to 1.5563 angstroms. EXAFS spectra were recorded at SRS stations 8.1 and 9.2. Data were measured at room temperature unless stated otherwise.

3. Analysis

EXAFS data were background-subtracted using the authors' program PAXAS. Combined refinements were performed using the program P (Binsted *et al*., 1996). The Rehr and Albers approximation (Rehr and Albers, 1990) was used for multiple scattering paths. The simplest possible treatment of EXAFS DW terms was used. This involved assigning a parameter $A=2\sigma^2$ to 'blocks' of single-scattering distances (described by a range of distances and atomic numbers). Other than for the spinels, high-R blocks were pre-assigned a value, or set to a multiple of the shorter distance parameters, which were refined. Constraints were used to ensure that parameters for distances X-Y at edge X must equal parameters for Y-X at edge Y. Parameters for the legs of multiple scattering paths are interpolated from the single-scattering values by the program. Where multiple edges are available, this results in about three refined terms per spectrum. Positions, cell parameters and peak-profile parameters are as for a PD refinement. PD isotropic thermal factors are refined independently of those for EXAFS. This is clearly undesirable, but will require considerable effort to rectify. An EXAFS energy zero E_F is required for each spectrum. The amplitude reduction factor (AFAC) was set to 1 throughout.

4. Results and discussion

Cobalt blue: This material has a cubic (*Fm-3m*) spinel structure, in which cations occupy tetrahedral or octahedral sites in a nearly close-packed oxygen framework. There are 16 identical octahedral sites and 8 identical tetrahedral sites per unit cell. Oxygen occupies sites (*u*,*u*,*u*), where departure of *u* from ¼ determines the relative size of the cation sites. The composition is ideally $Co^{2+}Al_2O_4$, with Co occupying the tetrahedral sites. In practice, commercial production always involves an excess of Al_2O_3, as attempts to produce the pure end member lead to a pronounced darkening of the product. This could be explained by the presence of octahedral Co^{3+} or by the presence of an additional Co_3O_4 phase (where half of the octahedral sites are nominally occupied by Co^{3+}). Co_3O_4 has the same structure, but a smaller cell parameter, by .019 Å at 298K, which should be easily detectable by high-resolution neutron or X-ray powder diffraction. This is not observed. Powder neutron diffraction results for compositions between $Co_{0.78}Al_{2.28}O_4$ and the stoichiometric compound revealed a variable amount of Co (0.79 to 0.90) on the tetrahedral site and an Al_2O_3 impurity phase, but

produced no clear evidence for octahedral Co. Some octahedral Co would be expected if the tetrahedral site is Co-deficient. A combined EXAFS/X-ray PD study, using synchrotron image-plate data, clearly showed the presence of octahedral cobalt however. A refinement of the sample with a nominal composition of $Co_{0.78}Al_{2.28}O_4$ gave 0.807(7) Co[4] and 0.058(3) Co[6]. The octahedral cobalt content rose to 0.11 for the stoichiometric composition. Although charge-balance demands that most of the octahedral Co is divalent, the bond valence sum for the octahedral site (Altermatt and Brown, 1985) favours Co^{3+}. Small amounts of trivalent Co in the stoichiometric compound's octahedral site would allow for charge-transfer between the tetrahedral site, explaining the discolouration. Here however, it is simply intended to draw attention to the potential of combined EXAFS/PD refinements to obtain extremely accurate site occupancy factors under favourable conditions, which in this case is due to the pronounced signature of Co[4]-Co[6] distances on both single and multiple scattering paths.

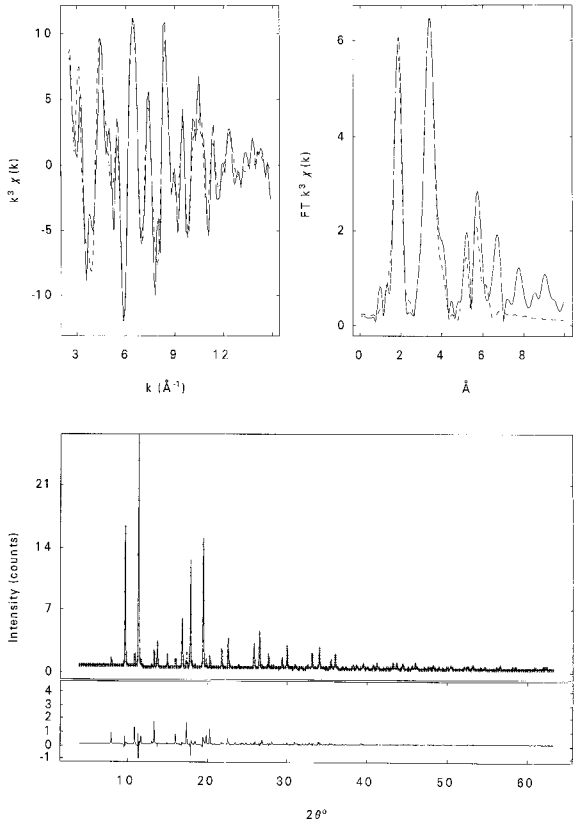

Figure 1
Fit to the Co K-edge EXAFS (above) and X-ray diffraction data (below) of $Co_{0.78}Al_{2.22}O_4$. TheAl_2O_3 impurity phase has not been fitted.

$La_{6.4}Ca_{1.6}Cu_6Ni_2O_{20}$: This compound is derived from the ideal cubic perovskite structure ABO_3, in which oxygen and the large 12 coordinated A cation form a cubic close packed framework, where the smaller B cations occupy octahedral holes. Here however, the structure is oxygen deficient, the ordered oxygen vacancies giving rise to an 8-8-20 superstructure with Cu and Ni occupying 4, 5 and 6 coordinated sites rather than just octahedral sites. The data showed the cations to be ordered with Ni in the octahedral sites. The usual 8-8-20 space group, *P4/mbm*, did not give a good fit to the EXAFS, and *P4/m* was used, which also improved the fit to the PND data. Comparison with the model compounds $La_2Ni_2O_5$ and $LaNiO_3$, showed the Ni XANES to resemble the Ni^{3+} compound, but with an edge position 1eV lower. This is consistent with the average oxidation state of 2.80 obtained by assuming all the Cu is present as Cu^{2+}. The fit obtained (table 1, fig. 2) gave EXAFS and PND reliability factors; R_{exafs} = 23.6 and R_{wp} = 7.48 respectively. Unit cell dimensions were a = 10.7319(3) Å and c = 3.8674(1) Å. The bond-valence sum for the Cu sites was consistent with Cu^{2+}. One Ni site was consistent with Ni^{3+}, the other with an intermediate 2+/3+ value. A major discrepancy is that the Debye-Waller term for ~3.9 Å Cu-Cu distances (A=0.019) was almost twice that of similar Cu-Ni distances. This is physically implausible. Constraining the DW terms produced a significantly worse fit. The reason for this is now understood, following a study of $La_{6.4}Ca_{1.6}Cu_7CoO_{20}$ (Binsted *et al.*, 2001). In this compound, provisional refinements show off-centre Cu[4] atoms, associated with distortion of the square planar sites. In cuprate superconductors, similar distortions have been ascribed to Jahn-Teller distortions. The local space group is then *P1*, but the long-range space group is *P4/mbm*. It is believed that the same effects will be found for the Ni compound, with locally ordered lattice distortions of a *P4/mbm* structure.

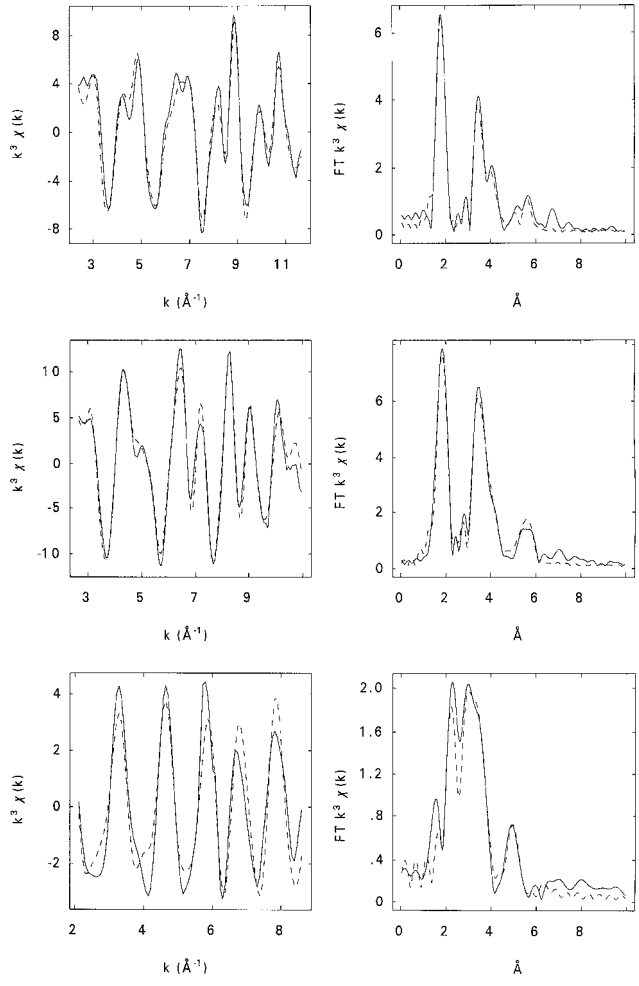

Figure 2
Fit to the Cu K-edge EXAFS (above), Ni K-edge EXAFS (middle) and La L_{III}-edge (below), using a *P4/m* model.

Table 1
P4/m coordinates for $La_{6.4}Ca_{1.6}Cu_6Ni_2O_{20}$

Label	x,y,z	Wyckoff no.	Coord.	$B_{isotropic}$
La/Ca1	.2549(19),.4656(16),.5	4k	10	0.36
La/Ca2	.0279(16),.2353(11),.5	4k	10	0.36
Ni1	.0,.0,.0	1a	6	0.24
Ni2	.5,.5,.0	1c	6	0.24
Cu1	.0,.5,.0	2e	4	0.24
Cu2	.2763(13),.2191(13),0.	4k	5	0.24
O1	.0,.0,.5	1b		1.00
O2	.5,.5,.5	1d		1.00
O3	.0,.5,.5	2f		1.00
O4	.2886(18),.2269(15),.5	4k		1.00
O5	.1554(19),.0914(24),.0	4k		1.00
O6	.3736(14),.8787(7),.0	4k		1.00
O7	.4080(25),.3359(22),.0	4k		1.00

$Pr_{0.5}Sr_{0.5}FeO_{2.75}$: This compound shows the most dramatic differences between the local structure and long-range structure that have been observed (figure 3). Although the PND data can be adequately fitted using the cubic space group *Pm-3m*, this is certainly not the case for the Pr and Sr edges. For Pr, the maximum symmetry that can explain the data is orthorhombic. It is not possible to fit the EXAFS simply by offsite displacement of Pr. The possibility of small-scale orthorhombic twinning is being investigated.

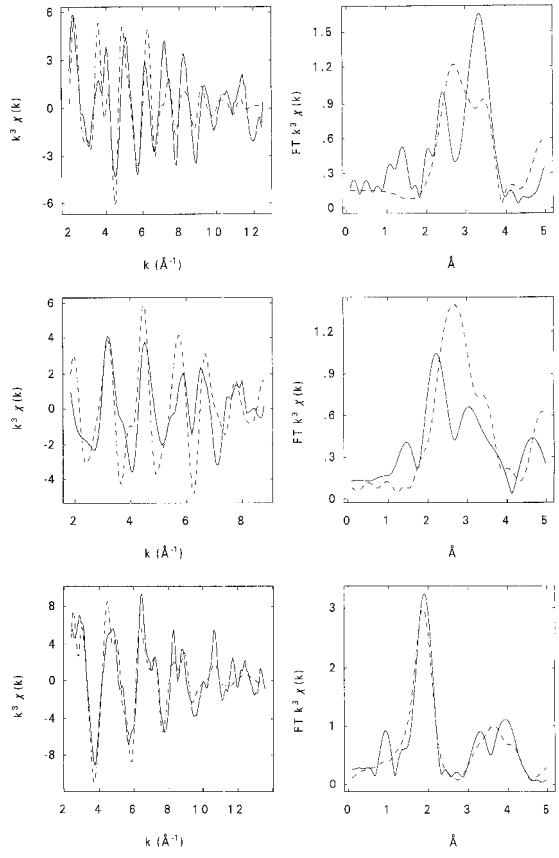

Figure 3
Fit to the Sr K-edge EXAFS (above), Pr L_{III}-edge EXAFS (middle) and Fe K-edge (below), using a cubic *Pm-3m* model.

In many of the systems that have been investigated, complex local effects are found to be important in understanding the structure. When it is necessary to introduce additional parameters to describe these effects, it is of course necessary to ensure that these do not exceed the information content of the data, but additional guidelines have proved useful. First of all it is important that changes to the model benefit both sets of data, and are not therefore compensating for systematic errors in one technique. Secondly, a useful test is to ensure that increasing the cluster size improves the fit to the EXAFS. This provides a more rigorous test of the model, without introducing additional parameters. This criterion has proved useful in finding discrepancies in the ordering of distortions. Thirdly, it is important that DW factors represent the true thermal contribution to the disorder. As in the example above, a proper understanding of the structure can only be obtained if static disorder is part of the model, rather than contributing to the DW factor. Clearly separation of thermal and static contributions would be best achieved using a single *ab initio* treatment of thermal effects for both techniques. This remains a goal for future development. Finally, it is important to establish that site geometry is realistic, and bond-valence sums are invaluable in this respect, as well as being helpful in assigning oxidation states if this is unknown.

Acknowledgments

This work has received financial support from the EPSRC, UK and the Research Council of Norway. The assistance of Lorrie Murphy, Fred Mosselmans and Mark Roberts, Daresbury Laboratory and Bjørn Hauback, IFE, Kjeller, are gratefully acknowledged.

References

Binsted, N., Pack, M., Weller, M. T., and Evans, J. (1996). *J.Am.Chem.Soc.***118**, 10200 –10210.
Weller, M. T., Pack, M. J. and Binsted, N. (1996). *Angew. Chem. Int. Ed.*, **37**, 1094-1097.
Binsted, N., Dann, S. E., Pack, M., and Weller, M. T. (1998),.*Acta Cryst*., **B54**, 558-563.
Binsted, N., Stange, M., Fjellvåg, H and Weller, M.T. (2001). Submitted to the proceedings of the LLD2K conference.
McGreevy, R. L. (1995). *Nucl. Instrum. Methods*, **A354**, 1-16.
Rehr, J. J. and Albers, R. C. (1990). *Phys. Rev.*, **B41**, 8139-8149.
Altermatt, D. and Brown, I. D. (1985). *Acta Cryst*., **41**, 240-244.

 Received 31 July 2000 • Accepted 14 December 2000